ILASS Americas, 18th Annual Conference on Liquid Atomization and Spray Systems, Irvine, CA, May 2005

Near-Field Characterization of Direct Injection Gasoline Sprays from Multi-Hole Injector Using Ultrafast X-Tomography

Xin Liu, Seong-Kyun Cheong, Christopher F. Powell, Jin Wang∗
Argonne National Laboratory, Argonne, IL 60439

David L.S. Hung, James R. Winkelman
Visteon Corporation, Van Buren Township, MI 48111-5711

Mark W. Tate[a], Alper Ercan[a], Daniel R. Schuette[a], Lucas Koerner[a], Sol M. Gruner[a, b]
[a]Department of Physics and [b]Cornell High Energy Synchrotron Source, Cornell University, Ithaca, NY 14853

Abstract

Detailed analysis of fuel sprays has been well recognized as an important step for optimizing the operation of direct injection gasoline engines to improve fuel economy and reduce emissions. However, the structure and dynamics of near-field multi-hole fuel injector sprays have not previously been visualized or reconstructed three dimensionally (3D) in a quantitative fashion. Using an ultrafast x-ray detector and intense x-ray beams from synchrotron radiation, the interior structure and dynamics of the direct injection gasoline spray from a multi-hole direct injector were elucidated for the first time by a newly developed, ultrafast computed microtomography technique. Many features associated with the transient liquid flows are readily observable in the reconstructed spray. Furthermore, an accurate 3D fuel density distribution was obtained as the result of the computed tomography in a time-resolved manner. These results not only reveal the near-field characteristics of the complex fuel sprays with unprecedented detail, but will also facilitate realistic computational fluid dynamic simulations in highly transient, multiphase systems.

∗ Corresponding author: wangj@aps.anl.gov

Introduction

As the worldwide demand for energy grows rapidly, the technologies capable of improving fuel efficiency and reducing emissions should play an essential role in the design of the new-generation automotive internal combustion engines [1]. Among these is gasoline direct-injection (GDI) technology, which has been the subject of research and development for a long time in the automotive industry. In a combustion system employing GDI, the fuel is directly injected into the combustion chamber instead of the air-intake port. Due to the ability to precisely control the injection rate, timing, and combustion of the fuel, the fuel efficiency and emission reduction potentials can be greatly improved [2].

The design of the fuel injector plays a key role in the performance of GDI engines. Generally, there are three types of fuel injector concepts for GDI engines, namely, swirl-type, slit-type, and multi-hole. Each concept has its own advantages. However, the multi-hole injectors are more promising because they offer the long sought spray pattern tailoring flexibility and reduced penetration [2-4]. Figure 1 depicts a prototype GDI injector and a representative nozzle. This injector utilizes a novel high-turbulence multi-hole nozzle to produce soft sprays with relatively well atomized droplets. Figure 2 shows a basic configuration of an 8-hole nozzle plate. In order to optimize the performance of such novel device, fundamental knowledge of the fuel sprays becomes extremely important.

Traditionally, quantitative fuel spray characterization in the close proximity of the injector tip has been difficult because it requires analysis of submillimeter-scale structures with microsecond time resolution in a complex multiphase flow. Despite significant advances in laser diagnostics in the past decade, the dense spray region close to the injector tip nozzle still has not yielded the desired quantitative information due to the inevitable problem of optical multiple scattering from the fuel droplets [5-7]. Recently, a new nonintrusive, quantitative, and time-resolved technique to characterize the dense part of fuel sprays has been developed based on monochromatic x-radiography/tomography technique [8-12]. Both techniques take advantage of high intensity and monochromaticity of the synchrotron radiation x-rays, which makes accurate quantitative measurement of highly transient fuel sprays with a time-resolved manner.

In this paper, we demonstrate the experiment of near-field multi-hole injector spray characterization using ultrafast x-tomography technique to quantitatively reveal the transient nature of pulsing spray. The prototype fuel injector used in this study has a modified 8-hole nozzle configuration to produce a wide-cone spray pattern. In addition, the hydraulic damping of the pintle movement has been slightly reduced such that after-injection dynamics (also known as spray bounce) can be made more pronounced. It is also our purpose to demonstrate how the ultrafast x-tomography technique can be applied to identify and measure spray bounce quantitatively. Some recent results of the quantitatively 3D reconstruction are presented with preliminary analyses.

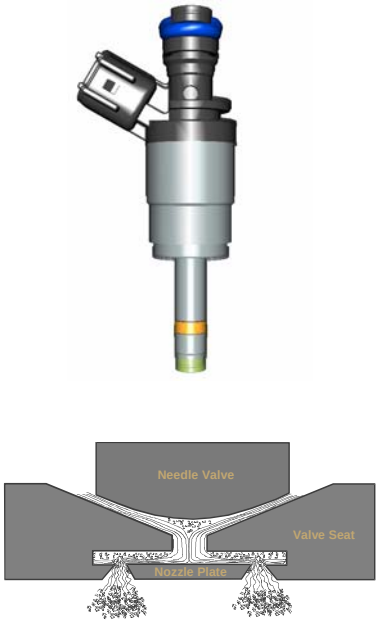

Figure 1. Prototype GDI fuel injector with a schematic of multi-hole turbulence nozzle [4].

Figure 2. Schematic of a basic 8-hole turbulence nozzle configuration.

Experimental Methods

The experiments are performed at the D-1 beamline of the Cornell High Energy Synchrotron Source (CHESS). Figure 3 shows the schematic experimental setup. The x-ray beam produced by synchrotron radia-

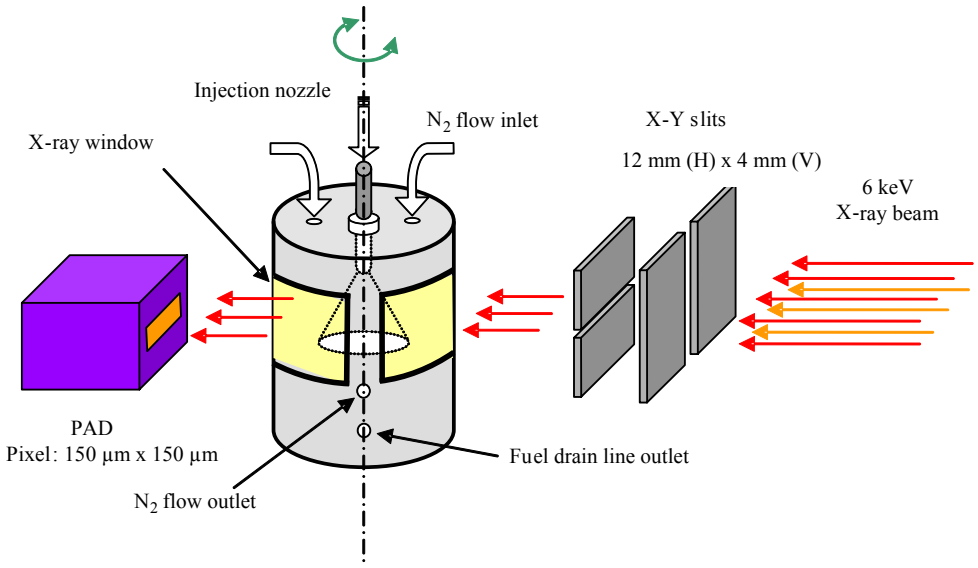

Figure 3. Schematic of experimental setup.

tion is monochromatized to 6.0 keV (with an energy bandwidth of about 1%) using a double-multilayer monochromator. This x-ray energy is optimal for probing the fuel, a blend of a calibration fluid and a cerium-containing fuel additive. The calibration fluid (Viscor 16-A) is a simulated fuel with properties similar to gasoline fuel with precisely controlled viscosity and specific gravity specifications. The monochromized beam was further collimated by a set of slits to 12 mm (H) x 4 mm (V).

The key component in the setup is the integrated tomography fuel chamber system which includes spray injection chamber, rotation and translation stages. The injection chamber is intended to provide environment enclosure for the fuel sprays. As shown in Fig. 3, there are two identical X-ray transparent windows situated symmetrically on the chamber with a 120° x-ray viewing angle. The windows are 6.5 cm high and are covered with polymer thin films. The injector is mounted on the top of the chamber as shown in Fig. 3. The injection pressure is set at 2 MPa and the nominal pulse duration of the spray is 2.5 ms (1.5 ms net pulse duration with a 1 ms pre-charging duration). Also fit to the chamber are two inlets and one outlet for flowing nitrogen gas through the chamber to scavenge the fuel vapor. On the side of the chamber, there is also a fuel drain line. The environment in the spray chamber is maintained at a pressure of 0.1 MPa and at room temperature (25-30°C in the radiation enclosure).

The spray chamber is designed to rotate and to translate in precise steps while the x-ray source and the detector are stationary. In this system, we use a horizontal rotational stage and a vertical translational stage to rotate the spray chamber and to select the slice to be imaged in the vertical direction. The minimum rotation angle is 0.0025°, and the minimum step size for the translation stage is 1.27 µm. All the rotational and translational stages are motorized. During the experiment, the parallel x-ray beams penetrate the spray at a given view angle θ, and after completion of the scans in temporal steps, the injection nozzle rotates a small angle $\Delta\theta$ and the temporal scan are repeated. This process is continued until the completion of 180° rotation.

Another important component in the setup is the ultrafast x-ray detector – Pixel Array Detector (PAD), which is developed at Cornell University [13, 14]. The pixel size of the PAD is 150 µm x 150 µm. The single imaging area is 92 (H) x 40 (V) pixels defined by the x-ray beam size. The complete imaging area is built up by shifting the position of the injector relative to the beam

Parameters	Quantity and Properties
Injection system	Visteon GDI, 8-hole nozzle
Outer diameter	3.0 mm
Fill gas	N_2, 0.1 MPa, 25 ~ 30 °C
Fuel	Viscor with Ce-additive
Specific gravity	857.7 mg/cm^3
Spray duration	2.5 ms (nominal)
Injection pressure	2 MPa
Region of interest	0 ~ 6 mm from the nozzle

Table 1. Experimental conditions.

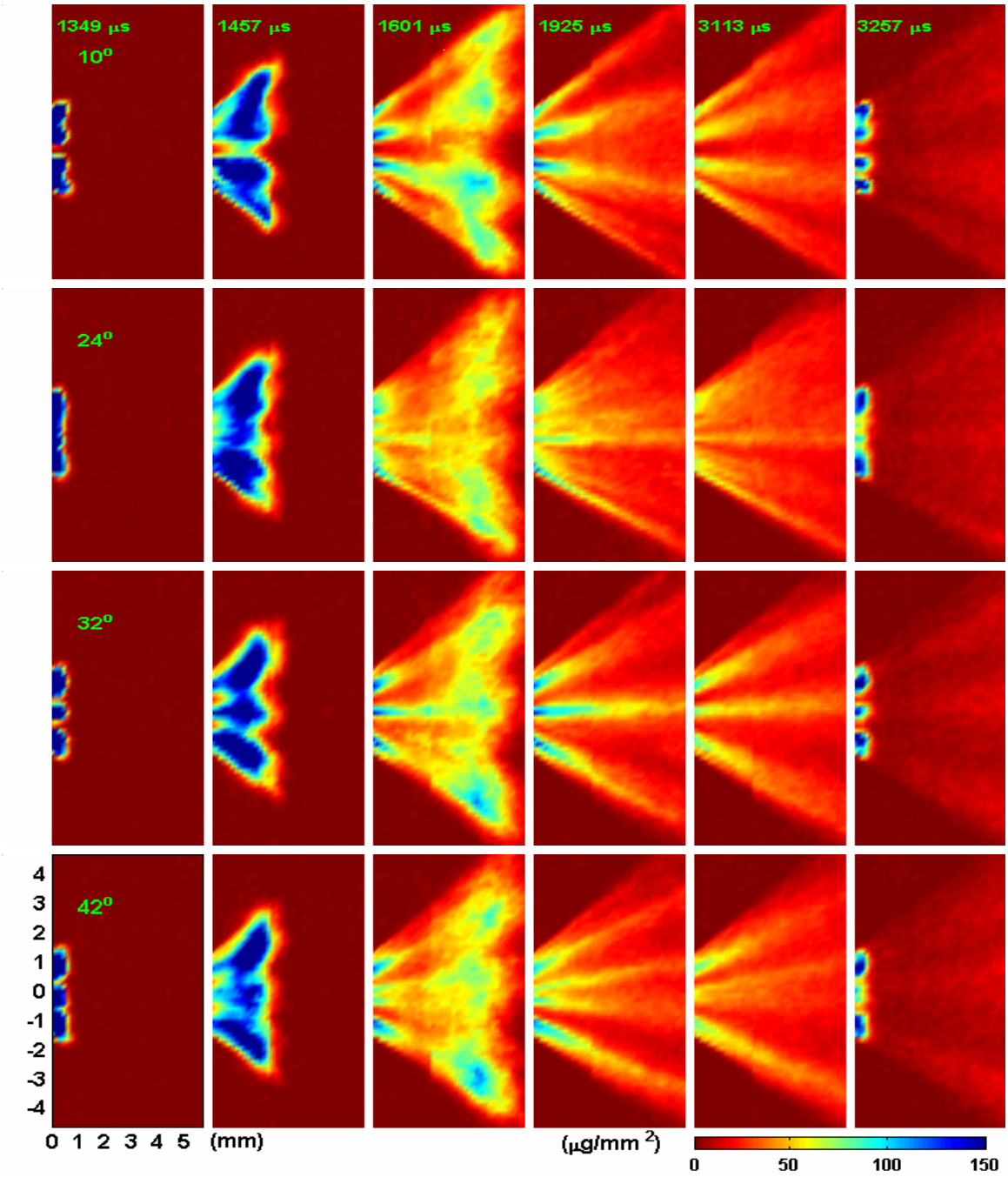

Figure 4. X-radiography images of 8-hole nozzle spray at selected angles and time instances.

and the PAD. During the experiment, the spray is triggered at 1.15 Hz and a series of frames is taken at various delay times. The exposure time per frame is set to 10.25 µs with an interval between frames of 25.6 µs. Each image is obtained by averaging 20 fuel-injection cycles. The complete experiment conditions are listed in table 1.

Results and Discussions

The images of the GDI sprays recorded by PAD at selected projection angles and time instances are shown in Figure 4. These images show the progression of the spray with unprecedented details. Different phases of the transient spray characteristics including the "sac", streak, and "bounce" can be readily observed. The rep-

resentative instances selected here are 1349 μs, when the spray tip just appeared at the nozzle; 1457 μs, when the "sac" portion was exiting the nozzle; 1601 μs, when the spray cone fully opened and "sac" portion started to break up with the main spray; 1925 μs, when the spray became stabilized; 3113 μs, just after the nozzle was closed; and 3257 μs, when the first "bounce" occurred. The sac spray is usually caused by the residual fuel trapped between the valve seat and the orifice holes during spray pulses, whereas the spray bounce can be associated with the hydraulic damping characteristics of the pintle movement. Even though both sac and bounce sprays are of much shorter duration in comparison to the main sprays, they could adversely affect the balance of air fuel mixing in the combustion processes.

Some basic characteristics of the sprays can be measured from these high contrast radiography images, such as spray penetration, fully developed cone angle, etc. Figure 5 shows the spray penetration versus time. More importantly, quantitative information, such as mass flow rate, total mass of "sac" and "bounce", etc., can be derived from these images thanks to the monochromatic x-rays. Based on the attenuation law, the 2D fuel mass density (with a unit of *mass*/*length-scale*^{2}) can be obtained by,

$$M = \frac{1}{\mu_M} \ln(\frac{I_o}{I}), \qquad (1)$$

where I_o and I are incident and transmitted x-ray intensities, respectively; μ_M is the mass attenuation coefficient of the fuel, which can be calibrated accurately.

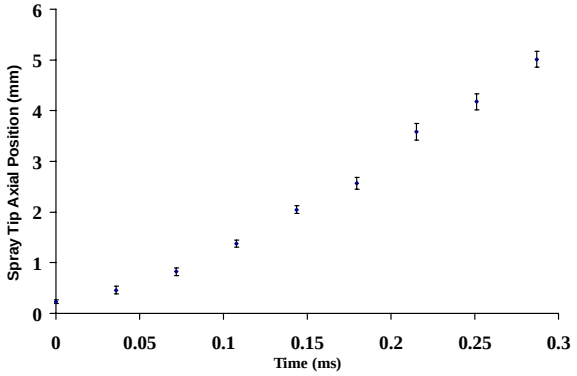

Figure 5. Spray penetration versus time. (Note: the time was shifted such that the initial spray tip appeared at time zero.)

Furthermore, from these projection images, the spray cross-section can be reconstructed in a three dimensional perspective by the computerized tomography technique. The principles of transmission tomography show that the linear attenuation coefficient distribution of the spray cross-section, $\mu_L(x, y)$, can be reconstructed from values of its line integrals provided the x-ray energy is monochromatic [15]. For our case, the line integrals of $\mu_L(x, y)$ can be easily resolved from the radiography images as shown in Fig. 4. With these line integrals (or "sinogram" – a nomenclature in tomography technique to describe a collection of line integrals form different angles), $\mu_L(x, y)$ is computed by several numerical methods based on filtered back-projection (FBP), algebraic iteration, and Fourier transform method. Fourier transform method was selected as our working algorithm due to its computation efficiency and relatively easy implementation. And, total of 180 projections were used to perform the reconstruction to maintain the spatial resolution near 150 μm. The fidelity of the reconstruction was also verified [11].

Finally, the fuel density distribution, $\rho(x, y)$, can be derived based on the following simple correlation,

$$\rho(x, y) = \frac{\mu_L(x, y)}{\mu_M}. \qquad (2)$$

The 3D fuel density distribution is, then, built upon all the reconstructed cross-sections at different locations.

Tomographic reconstruction is a great improvement over radiography imaging. The flow pattern of the multi-hole sprays has been revealed in a highly quantitative manner, which is very difficult by other means. Consequently, quantitative characterization of each jet from the multi-hole nozzle has been realized. Figure 6 shows the reconstructed fuel density distribution of a single slice at different positions. This figure indicates that all eight jets from different holes can be clearly identified. Although the shape of the jet is somewhat irregular, it always appears that a relatively dense core region is surrounded by a cloudy liquid-vapor mixture, which is not axial symmetrical. Although the sprays come out of a symmetrical multi-hole nozzle configuration, the axially asymmetric fuel distribution could be caused by slight radial movement of the pintle and manufacture imperfection of the nozzle orifices. Figure 7 shows a time series of the cross-sectional fuel-density distribution at 2.4 mm from the nozzle. These cross sections represent the density distribution of "sac", stabilized spray, spray after nozzle closed, and the first "bounce" of the pintle. This figure shows that the spray pattern and density changes greatly in time.

From the sequence of these reconstructed images, the progression of the spray was revealed with unprecedented details. As shown in Fig. 8, a time-evolution of a

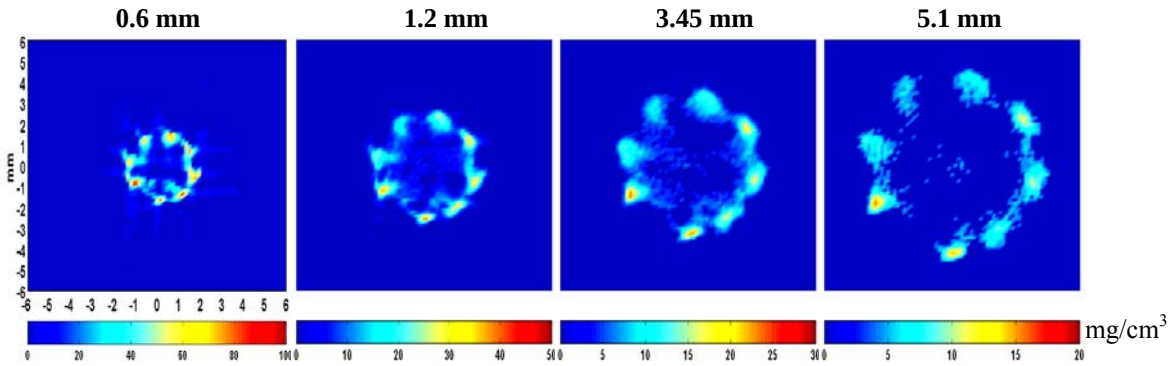

Figure 6. Reconstructed fuel density distribution at 2717 μs at different locations from nozzle.

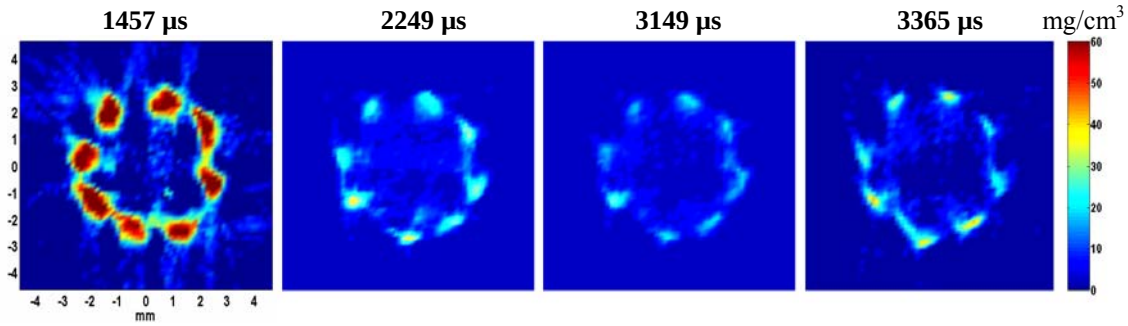

Figure 7. Fuel density distribution at 2.4 mm form nozzle at different time.

selected single jet dense core was plotted. This figure indicates that the spray started with a "sac" after the needle valve lifted. Immediately after the "sac", there was a very short time fluctuation, which indicates the "sac" portion is broken up from the succeeded sprays at this location (0.6 mm away from the nozzle), and isolated from the main spray later due to hydrodynamic instability. The main spray is relatively steady and multiple "bounce" was also observed when the pintle was closing. The quantitative characteristics of spray bounces can therefore be extracted accurately in comparison to the other phases of the spray pulse. This should provide a good insight on optimizing the hydraulic damping of the injector to minimize any after-injections during the closing of the pintle.

Study of individual jet characteristics and jet-to-jet variation are very important to design and optimize multi-hole nozzles. With the quantitative 3D reconstruction, considerable information can be obtained, such as jet velocity (vector), jet diameter, mass flux, density, etc. Figure 9 shows the dense-core density of each spray at steady state as a function of downstream distance. The fuel density at nozzle exit is much less than the liquid fuel density (857.7 mg/cm^3), indicating that the fuel has already undergone atomization. Within a few millimeters, the density falls off rapidly from ~120 mg/cm^3 to ~20 mg/cm^3.

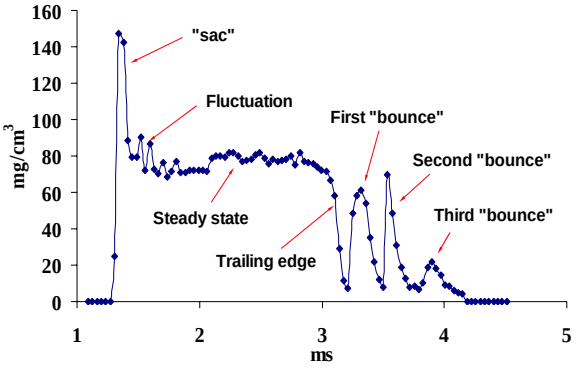

Figure 8. Time-evolution of a single jet density at 0.6 mm from nozzle.

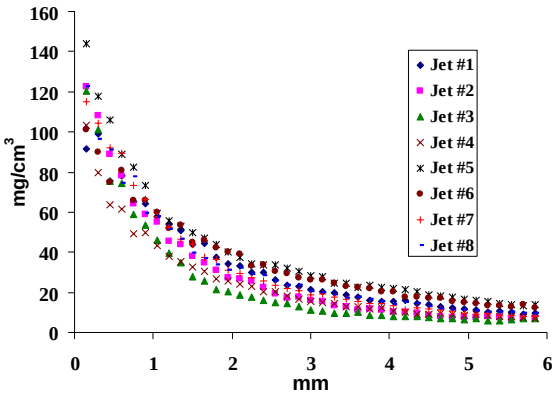

Figure 9. Falloff of single jet peak density along the spray axis. The data represent the fuel density at 2.7 ms after the start of the injection during the more steady portion of the injection process.

Summary

In this paper, we have described the use of monochromatic x-tomography to study the near-field multi-hole GDI sprays in a highly quantitative and time-resolved manner. The time-evolution of the sprays is directly imaged with microsecond resolution, and the internal structure of the multi-hole spray is fully reconstructed quantitatively with submillimeter spatial resolution. The preliminary results indicate that the core region near the nozzle is composed of a liquid/gas mixture with a density much less than of the bulk liquid fuel density. This technique allows the quantitative determination of several key characteristics of the transient sprays such as the "sac" and the pintle bounce. With the ongoing investigations, more information about single jet characteristics and jet-to-jet variations can also be derived. The information obtained should benefit the theoretical simulation of multi-hole spray process in this region. The success of the measurements has demonstrated that the x-tomography technique is well suited for the multi-hole spray characterization in the close proximity of the injector tip. We believe that this technique can be used as a sensitive probe and diagnostic tool for investigating other highly transient phenomena.

Acknowledgements

The authors are thankful to Bob Larson for his support in this research. The work and the use of APS (1-BM beamline) are supported by the U.S. Department of Energy under contract W-31-109-ENG-38 through an Argonne National Laboratory LDRD grant. The authors wish to acknowledge the technical support from Visteon Corp. And the authors also would like to thank the staff at APS 1-BM beamline and the staff at CHESS, funded by the U.S. National Science Foundation (NSF) and the U.S. National Institute of General Medical Sciences via NSF under award DMR-9713424. PAD detector development was funded by DOE grants DE-FG-0297ER14805 and DE-FG-0297ER62443.

References

1. Cohn, D.R., and Heywood, J.B., *Physics Today* 55:12-13 (2002).
2. Zhao, F., Lai, M.-C., Harrington, D.L., *Progress in Energy and Combustion Science* 25:437-562 (1999).
3. Xu, M., Porter, D.L., Daniels, C.F., Panagos, G., Winkelman, J.R., Munir, K., SAE 2002-01-2746.
4. Hung, D.L.S., Mara, J.P., Winkelman, J.R., *ILASS Americas, 17th Annual Conference on Liquid Atomization and Spray Systems*, Arlington, VA, May 2004.
5. Adrian, R.J., *Ann. Rev. Fluid Mechanics* 23:261-304 (1991).
6. Coil, M.A., and Farrell, P.V., SAE 950458.
7. Sick, V., and Stojkovic, B., *Applied Optics* 40:2435-2442 (2001).
8. Powell, C.F., Yue, Y., Poola, R., Wang, J., *J. Synchrotron Rad.* 7:356-360 (2000).
9. MacPhee, L.E., Tate, M.W., Powell, C.F., Yue, Y., Renzi, M.J., Ercan, A., Narayanan, S., Fontes, E., Walther, J., Schaller, J., Gruner, S.M., Wang, J., *Science.* 295:1621-1622 (2002).
10. Cai, W., Powell, C.F., Yue, Y., Narayanan, S., Wang, J, Tate, M.W., Renzi, M.J., Ercan, A., Fontes, E., Gruner, S., *Applied Physics Letters* 83:1671-1673 (2003).
11. Cheong, S.-K., Liu, J., Shu, D., Wang, J., Powell, C.F., SAE 2004-01-2026.
12. Liu, X., Liu, J., Li, X., Cheong, S.-K., Shu, D., Wang, J., Tate, M.W., Ercan, A., Schuette, D.R., Renzi, M.J., Woll, A., Gruner, S.M., *49th Annual Meeting of SPIE*, (invited) Denver, CO, August 2004, 5535:21-28.
13. Barna, S.L., Shepherd, J.A., Tate, M.W., Wixted, R.L., Eikenberry, E.F., Gruner, S.M., *IEEE Trans. Nucl. Sci.* 44:950-956 (1997).
14. Rossi, G., Renzi, M., Eikenberry, E.F., Tate, M.W., Bilderback, D., Fontes, E., Wixted, R., Barna, S.L., Gruner, S.M., *J. Synchrotron Rad.* 6:1096-1105 (1999).
15. Kak, A.C., and Slaney, M., *Principles of Computerized Tomographic Imaging*, IEEE Press, New York, 1999.